

Research Article

Detailed and atypical HLA-E peptide binding motifs revealed by a novel peptide exchange binding assay

Lucy C. Walters, Andrew J. McMichael and Geraldine M. Gillespie 

Nuffield Department of Medicine Research Building, Roosevelt Drive, Nuffield Department of Medicine, University of Oxford, Oxford, UK

Diverse SIV and HIV epitopes that bind the rhesus homolog of HLA-E, Mamu-E, have recently been identified in SIVvaccine studies using a recombinant Rhesus cytomegalovirus (RhCMV 68-1) vector, where unprecedented protection against SIV challenge was achieved. Additionally, several *Mycobacterial* peptides identified both algorithmically and following elution from infected cells, are presented to CD8⁺ T cells by HLA-E in humans. Yet, a comparative and comprehensive analysis of relative HLA-E peptide binding strength via a reliable, high throughput in vitro assay is currently lacking. To address this, we developed and optimized a novel, highly sensitive peptide exchange ELISA-based assay that relatively quantitates peptide binding to HLA-E. Using this approach, we screened multiple peptides, including peptide panels derived from HIV, SIV, and Mtb predicted to bind HLA-E. Our results indicate that although HLA-E preferentially accommodates canonical MHC class I leader peptides, many non-canonical, sequence diverse, pathogen-derived peptides also bind HLA-E, albeit generally with lower relative binding strength. Additionally, our screens demonstrate that the majority of peptides tested, including some key Mtb and SIV epitopes that have been shown to elicit strong Mamu-E-restricted T cell responses, either bind HLA-E extremely weakly or give signals that are indistinguishable from the negative, peptide-free controls.

Keywords: CD8⁺ T cells · epitope motif · HIV · HLA-E · *Mycobacterium tuberculosis*



Additional supporting information may be found online in the Supporting Information section at the end of the article.

Introduction

It is well established that HLA-E preferentially accommodates a signal peptide comprising residues 3–11 of MHC class Ia leader sequences, typically VMAPRT (L/V)(V/L/F)L (VL9), in its binding groove and that these peptides dominate the HLA-E-presented ligandome in the steady state [1,2]. VL9 peptide-bound HLA-E complexes constitute major ligands for heterodimeric inhibitory CD94-NKG2A and activating CD94-NKG2C receptors predomi-

nantly expressed on NK cells. VL9-bound HLA-E-CD94/NKG2A engagement has been shown to regulate NK cell-mediated lysis and represents an important component of immune homeostasis [3,4,5].

In the original peptide binding studies, the HLA-E sequence motif was explored via Ala and Gly substitution experiments along the HLA-B*0801 leader peptide (VMAPRTVLL), for which strong sequence selectivity was uncovered at primary anchor positions 2 (Met) and 9 (Leu), with weaker preferences observed for secondary anchor positions 7 (Val) and 3 (Ala) [1]. Subsequent structural characterization of HLA-E revealed unusually high binding pocket occupancy compared to classical MHC class Ia molecules. In addition to the peptide's primary anchor side chains at positions

Correspondence: Prof. Geraldine M. Gillespie and Dr. Lucy C. Walters
e-mail: geraldine.gillespie@ndm.ox.ac.uk; lucy.walters@ndm.ox.ac.uk

2 (Met) and 9 (Leu) that project into their respective B and F pockets, positions 3 (Ala), 6 (Thr), and 7 (Val/Leu) also constituted secondary anchor residues, with their side chains occupying the shallow D, C, and deeper E pockets, respectively [6–8]. The shape complementarity of these side chains, in addition to pocket-based interactions such as hydrogen bonding, van der Waals, and hydrophobic contacts place sequence restrictions on the peptide in these various anchor positions, reducing the overall magnitude of the potential peptide binding repertoire [9]. It was argued therefore that the requirement to occupy a greater number of pockets, as observed in VL9-bound structures of HLA-E, would correlate with a less diverse peptidome than classical MHC class I allotypes [6]. However, non-VL9 sequence-diverse peptides that bind HLA-E or its rhesus or murine orthologs, Mamu-E or Qa-1, respectively, have subsequently been identified in diverse immunological settings. For example, HLA-E- and Qa-1-restricted peptides from pathogens including *Salmonella* [10,11], Hepatitis C virus [12], EBV [13], and Influenza virus [13], have been reported. These findings also extend to self-derived peptides from proteins such as Fam49B [14], Hsp60 [15], and Prdx5 [16] in the context of defective antigen processing, cellular stress, or autoimmune disease.

More recently, two contexts where large numbers of MHC-E-restricted epitopes are presented have been reported—vaccination of rhesus macaques with a RhCMV 68-1 vector recombinant for SIV or HIV antigen [17] and *Mycobacteria tuberculosis* (Mtb) infection, BCG vaccination, or environmental *Mycobacterial* exposure [18,19]. Importantly, Mamu-E-restricted CD8⁺ T cell responses have been implicated as immune correlates of unprecedented protection against SIV challenge in RhCMV68-1 vector vaccination studies in rhesus macaques [17]. However, these Mamu-E-restricted epitopes are sequence-diverse, contain non-canonical anchor residues and lack a common motif [17]. Notably, despite a considerable degree of sequence divergence between the human and rhesus MHC-E homologs, heavy chain-derived residues forming the B, D, C, E, and F pockets of the binding groove exhibit strong sequence conservation [20]. Given this stringent sequence conservation between pocket-forming residues, it is likely these homologs share a largely overlapping peptide binding repertoire. In the second predominant setting, 69 *Mycobacterial* peptides were predicted to bind HLA-E in silico using peptide motif-based algorithms, of which 55 were shown to stimulate HLA-E-restricted CD8⁺ T cell responses in PPD-responding individuals [18]. A smaller set of HLA-E-restricted Mtb-derived peptides were more recently eluted from infected cells and validated as CD8⁺ T cell epitopes [21].

Given the identification of a large number of non-VL9 pathogen- and self-derived HLA-E-binding peptides, we recognized the need to develop an assay to reliably and comparatively assess the HLA-E peptidome. We therefore designed and optimized a new in vitro peptide exchange ELISA-based assay to validate and relatively quantitate peptide binding to HLA-E. Although we previously validated HLA-E peptide binding [17] using a micro-refolding ELISA-based assay, originally developed to determine peptide binding affinity to classical MHC class I molecules [7,22],

this assay suffered from variability between biological repeats, so that very large numbers of replicate assays were required to achieve statistically robust results. The variability was likely caused by assay-to-assay fluctuations in protein refolding in addition to unusually high background signals, due to partial HLA-E-β2M refolding in the absence of added peptide [20]. To improve the system, we adopted a new UV peptide exchange ELISA-based assay (Fig. 1A) [23]. In this assay, HLA-E heavy chain and β2M are pre-refolded with a UV-labile HLA-E binding peptide based on the VL9 sequence in which the solvent exposed Arg at position 5 of VL9 was replaced with a photo-cleavable, unnatural 2-nitrophenylamino acid residue [20,23]. Such conditional peptide ligand technology was originally developed for HLA-A*02:01 [23] and subsequently adapted to facilitate peptide exchange in HLA-A*1, -A*3, -A*11, -B*7, and -B*57 molecules [24,25]. Specifically, the nitrophenyl moiety within the substituted beta amino acid is sensitive to UV illumination at >350 nm. This results in peptide cleavage and successive dissociation of the degraded peptide fragments from the MHC class I peptide binding groove, as previously validated by mass spectrometric analysis [23]. Consequently, in the absence of bound peptide, MHC class I complexes become destabilized and disintegrate. However, complex disintegration can be circumvented by peptide exchange with a rescue peptide that binds the MHC allele in question.

Using this approach both pathogen- and self-derived peptides previously reported to bind HLA-E were screened. Our results indicate that although HLA-E preferentially accommodates MHC class I leader peptides, a range of other peptides containing hydrophobic and polar primary anchor residues are also tolerated, albeit with lower binding strength relative to VL9 peptides. Importantly, our screens also demonstrate that the majority of peptides tested, including some key Mtb and SIV epitopes that have been shown to elicit immunodominant MHC-E-restricted T cell responses, bind HLA-E extremely weakly, or generate indistinguishable signals from the no peptide negative controls. Finally, while the stronger binding peptides show a clear sequence motif that could help identify further antigenic peptides, many of the well-defined peptide epitopes lack a motif suggesting that alternative peptide binding modes may exist for these peptides in vivo.

Results

UV peptide exchange HLA-E binding assay optimization

Optimization of UV peptide exchange ELISA-based assay buffer system

Three distinct buffer systems were trialed in the photo-assisted peptide exchange reaction including a Lutrol-Tris-maleate-based buffer previously used in the micro-refolding peptide binding assay [22,7,20], a Tris-based buffer previously used for UV-induced peptide exchange with classical MHC class I molecules [23],

and finally an L-arginine-Tris-based buffer traditionally used in macro-refolding of class I MHC proteins [26] (Fig. 1B). The L-arginine-Tris-based buffer yielded lower peptide-free background signals, concomitantly improving peptide to background ratios for all peptides tested. As the peptide to background ratios were superior when the peptide exchange reaction was conducted in the L-arginine-Tris-based buffer, this buffer was subsequently adopted for follow-up.

To determine which component of the L-arginine-Tris-based buffer was responsible for reduced peptide-free background signals, further assays were carried out in which L-arginine monohydrochloride or the glutathione redox components were individually excluded (Fig. 1C). In the absence of L-arginine monohydrochloride, the average absorbance signal for the peptide-free background increased from 0.18 to 0.65, whereas, in the absence of the redox system the background signal remained unaffected at 0.18. Such results indicate that L-arginine monohydrochloride is the reagent responsible for peptide-free background reduction. To further evaluate the effect on the background signal, the concentration of L-arginine monohydrochloride was titrated and an inverse correlation was observed between L-arginine monohydrochloride concentration and the average absorbance reading of the peptide-free negative control (Fig. 1D). As lower peptide to background ratios, including those for the positive control VL9 peptide, were also observed at increasing L-arginine monohydrochloride concentrations, 400 mM was chosen as the optimal concentration for subsequent assays.

UV exposure versus no-exposure optimization

The recommended duration of UV exposure in previously published protocols using UV-labile ligand technology is 1 h [23]. However, we hypothesized that extended exposure could enable further cleavage of UV-sensitive peptides resulting in enhanced destabilization of HLA-E complexes in the absence of rescue peptide that should, in turn, further reduce background signals and improve peptide to background ratios. We therefore exposed the peptide exchange reaction to UV radiation for 0, 1, or 2 h before sampling by sandwich ELISA (Fig. 2A). As predicted, the peptide to no rescue background ratios of both test peptides, RL9HIV (RMYSPTSIL) and RL9SIV (RMYNPTNIL), and the positive control VL9 peptide were higher after 2 h of UV exposure. Further investigation revealed that peptide to background ratios of both test peptides and the positive control VL9 were similar after 2 or 3 h of UV exposure and began to decrease at the 4 h UV exposure time-point, perhaps due to radiation damage reducing overall protein yield in the reaction (Fig. 2B).

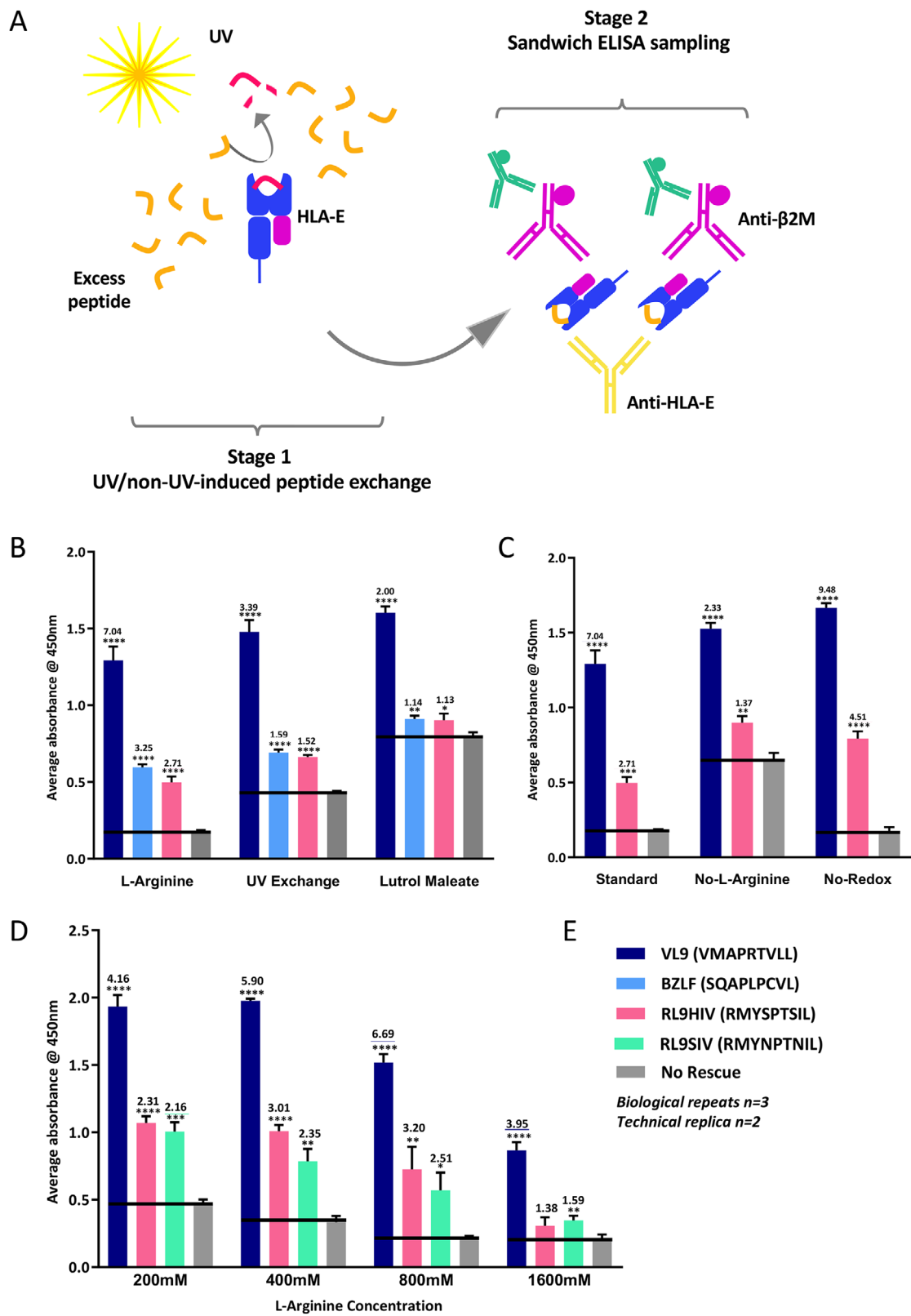
However, it remained uncertain whether this increased assay sensitivity was attributable to prolonged photo-irradiation or simply due to the extended time period over which peptide exchange could occur. Although exposure to light within the UV spectrum was originally deemed necessary for photo-cleavage and resultant exchange of HLA-A2.1-restricted UV-labile peptides [23], this had

not been fully elucidated for the UV-labile HLA-E binding peptide (VMAPIITLV) [20]. Also, since we previously observed unassisted peptide exchange in the blue native gel system where pre-refolded VL9-bound HLA-E incubated in the presence of excess Mtb44 was capable of converting to Mtb44 peptide-loaded material [20] (evidenced by distinct Blue Native gel band positioning), experiments to test the possibility of UV-independent peptide exchange were therefore conducted (Fig. 2C). Both in the presence or absence of UV irradiation we observed similar data trends for test peptide to background ratios over time-points of 0–3 h indicating peptide exchange did not require targeted UV illumination at 366 nm. However, in contrast to photo-illuminated peptide exchange reactions, test peptide to background ratios increased beyond the 3 h time-point in the absence of UV. An optimal duration of 5 h was thus selected as standard for the non-UV peptide exchange reaction.

Micro-refolding versus peptide exchange HLA-E binding assay comparison

We conducted a direct comparison of the previously published HLA-E micro-refolding [20,7] versus the novel peptide exchange binding assays to determine which approach yielded the highest sensitivity and reliability in discriminating weak HLA-E peptide binders from background signals (Fig. 3). Three biological repeats for two test peptides, BZLF1 (SQAPLPCVL) and GroEL (KMLRGVNV) that were previously reported to support HLA-E or Qa-1 stabilization, were included in this comparison [13,10]. Notably, the hierarchy of relative peptide affinity remained constant across both approaches with the BZLF peptide exhibiting the strongest and GroEL the weakest binding to HLA-E. However, the average absorbance reading for each test peptide was statistically significant in the initial UV-induced peptide exchange assay, whereas only VL9 achieved significance in the micro-refold approach. Further, the SD between biological repeats was lower for all peptides tested including the positive and negative controls in the initial UV-induced peptide exchange assay compared to the micro-refold approach. The SD for three biological repeats of the “no peptide” negative control decreased by over an order of magnitude in the initial UV exchange approach compared to the micro-refold assay (from 0.49 to 0.02, respectively) (Fig. 3D).

Following assay optimization, greater statistical significance was achieved for both BZLF1 (SQAPLPCVL) and GroEL (KMLRGVNV) test peptides and the SD was further reduced relative to the non-optimized UV peptide exchange assay, except for the negative control that remained low at 0.02 (Fig. 3). Assay sensitivity, defined by an ability to discriminate between low affinity HLA-E peptide binding and the no-peptide background, was considerably improved post-optimization—the test peptide to background signal ratio for BZLF1 more than doubled in the optimised, non-UV peptide exchange assay relative to the initial UV exchange assay.



Screening of HIV-derived peptides predicted to bind HLA-E

Once optimization protocols for the peptide exchange ELISA-based assay were complete, panels comprising HIV-derived 9mer peptides were screened for their HLA-E binding capacity. The first panel consisted of 16 peptides identified in-house as HLA-E predicted binders using the NetMHC 4.0 web-based server [27,28] (Fig. 4A), and thus were biased by computational predications based on previously established HLA-E binding motifs. 11 of the predicted peptides had the canonical Leu at position 9, and 11 contained a hydrophobic residue at position 2. A range of relative binding affinities were observed for this panel, with 12 of the 16 peptides demonstrating significant binding to HLA-E, albeit with much lower strength compared to the VL9 control peptide. For example, five of the significant HLA-E binding peptides in this panel generated average absorbance readings below 5% of the positive control VL9 signal following background subtraction (Supporting Information Table S2).

A second panel comprising HIV Gag- and Pol-derived peptides, based on a simple prediction of canonical primary anchor position 2 Met and a hydrophobic primary anchor position 9 residue, was also screened (Fig. 4B). Although two peptides from this panel demonstrated significant binding above background, all peptides exhibited very low average absorbance signals, only slightly higher than the negative control peptide-free background and all below 5% of the positive control VL9 signal following buffer subtraction (Supporting Information Table S2).

Peptides containing overlapping HIV Gag 9mers comprised the third panel screened for HLA-E binding. Many of these peptides contained biochemically distinct, non-canonical primary and secondary anchor residues and would not qualify as HLA-E binding peptides based on previously established sequence motif algorithms. The majority of these peptides generated exceptionally low

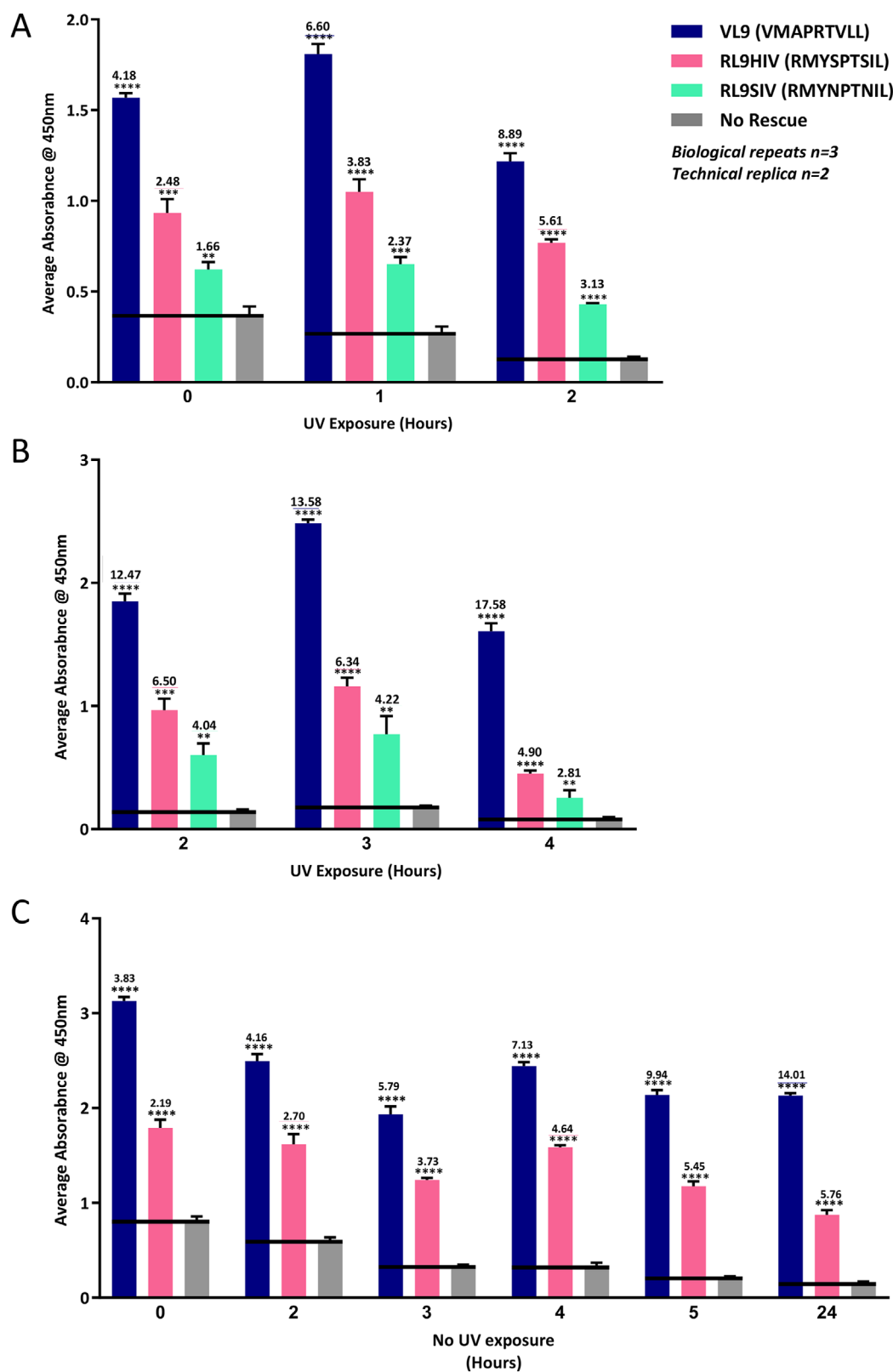
binding signals with average absorbance readings only marginally above the no rescue background signal (Fig. 4C–G).

The relative HLA-E peptide binding strength of a small peptide panel comprising the immunodominant SIV-derived RL9SIV (RMYNPTNIL: termed “supertope” because it elicits CD8⁺ T cell responses in all rhesus monkeys vaccinated by the RhCMV 68-1 vaccine [17]) and its HIV Clade B-derived alignment counterpart peptide, RMYSPTSIL (peptide ID: RL9HIV), was also evaluated (Fig. 4H). The physiological relevance of the RL9HIV peptide was validated by the identification of specific Mamu-E-restricted CD8⁺ T cell responses in rhesus macaques vaccinated with RhCMV 68-1 vectors recombinant for HIV Gag [20]. Although both RL9HIV and RL9SIV binding exhibited the greatest degree of statistical significance ($p \leq 0.0001$), the average absorbance signal for RL9HIV was consistently greater than that generated by RL9SIV; the RL9HIV average absorbance reading comprised 43% of the positive control VL9 signal, whereas RL9SIV was lower at 22% (Supporting Information Table S2).

Screening of Mtb-derived peptides predicted to bind HLA-E

A panel of *Mycobacterial* peptides eluted from Mtb-infected cells [21] was screened in the improved assay system (Fig. 5A). As these peptides were eluted from HLA-E, they were not subject to algorithmic bias from previously described HLA-E-restricted peptide sequence motifs. Peptides in this panel not only deviated from the canonical HLA-E sequence motif but also from the preferred nonameric peptide length. In addition to a peptide comprising 12 amino acids (GT12, GGILIGSDTLT), two nonameric Mtb peptides, IL9 (IMYNYPAML) and LL9 (LLDAHIPQL), with hydrophobic residues at both primary anchor positions demonstrated significant binding to HLA-E. The

Figure 1. UV-induced peptide exchange buffer optimisation. (A) Schematic representation of the novel UV/non-UV-induced peptide exchange ELISA-based method. In stage 1, β 2M-bound (violet) HLA-E (blue) pre-refolded and purified with the UV-labile VL9 variant peptide (VMAPI/TLVL) (magenta) is exposed to UV irradiation in the presence of excess test peptide. In the presence of UV-irradiation, the photo-sensitive VL9 peptide is cleaved and dissociates from the binding groove—this peptide also dissociates independent of photo-induced cleavage. A molar excess of test peptide (orange) enables peptide exchange. The peptide binding affinity of the rescue peptide (orange) determines the concentration of correctly refolded β 2M-bound HLA-E complexes in solution and in the absence of a rescue peptide the complexes dissociate. The relative concentration of β 2M-bound HLA-E complexes is determined indirectly via sandwich ELISA whereby a sample of the peptide exchange reaction is added to an ELISA plate pre-coated with the HLA-E-specific antibody 3D12 (yellow) in stage 2 of the assay. The subsequent addition of a horse radish peroxidase-coupled β 2M-specific detection antibody (violet) and subsequent antibody-enabled amplification (green) enables the detection of β 2M-bound HLA-E complexes-only. Reactions are developed with TMB and terminated with STOP solution prior to obtaining absorbance signals at 450 nm. (B) Average absorbance readings from 3 different buffer systems trialled in the UV-induced peptide exchange sandwich ELISA peptide binding assay. The Y-axis denotes average absorbance readings at 450 nm and the X-axis denotes the buffer system. Peptide to background ratios are indicated above each bar. (C) Average absorbance readings from three peptide binding ELISA optimization assays in which components of the L-arginine-based refolding buffer were individually excluded. The “standard” buffer contains all components of the L-arginine-based macro-refolding buffer (detailed in Materials and Methods). L-Arginine monohydrochloride was excluded from the “No L-Arginine” assay and the glutathione redox system excluded from the “No-Redox” assay. The Y-axis denotes average absorbance readings at 450 nm and the X-axis denotes buffer composition. Peptide to background ratios are indicated above each bar. (D) Average absorbance readings from peptide binding assays in which the L-arginine monohydrochloride concentration was varied in the UV-induced peptide exchange reaction from 200 to 1600 mM. The Y-axis denotes average absorbance readings at 450 nm and the X-axis denotes L-arginine concentration. Peptide to background ratios are indicated above each bar. (E) Shared Figure legend coloring throughout, with individual peptide IDs and sequences denoted. Peptide ID, sequence, origin, and corresponding references are detailed in Supporting Information Table S1, A (iv) and C. Positive control peptide VL9 (HLA-B7-derived leader sequence peptide VMAPI/TLVL) shown in dark blue with peptide free background (No rescue) in grey. Three biological repeats, namely, three individual peptide exchange reactions per test peptide were carried out simultaneously ($n = 3$), with two technical replicates sampled from the same peptide exchange reaction performed for each biological repeat (technical replica = 2). Stars above error bars reflect degree of significance in peptide binding by two-tailed t-tests (no star, $p > 0.05$, * $p \leq 0.05$, ** $p \leq 0.01$, *** $p \leq 0.001$, **** $p \leq 0.0001$). Error bars depicting SD of biological repeats are shown.



IL9 signal was particularly strong and represented 65% of the VL9 positive control signal following background subtraction (Supporting Information Table S2).

A small subset of the 69 previously published *Mycobacterial* peptides that were algorithmically predicted to bind HLA-E [18], were also screened (Fig. 5B). As these peptides were initially identified in silico based on previous sequence motifs, they are largely canonical with either a hydrophobic Leu or Met at position 2 and a hydrophobic Leu or Ile at position 9. One peptide, Mtb44 (RLPAKAPLL), exhibited strikingly strong binding, generating an average absorbance signal that comprised 97% of the VL9 positive control signal following buffer subtraction (Supporting Information Table S2) and represented the only non-VL9 peptide screened in the ELISA assay to generate an average absorbance reading within the SEM of the positive VL9 control. The second strongest binder, Mtb14 (RMAATAQVL), generated average absorbance readings between 40 and 50% of the positive control signal following background subtraction and contained the canonical primary anchor residues Met at position 2 and Leu at position 9 (Supporting Information Table S2). Although all peptides in this panel generated average absorbance signals above background levels in the peptide exchange assay, Mtb54 (FLLPRGLAI), Mtb48 (RLANLLPLI), and Mtb55 (VMATRRNVL) generated lower binding signals, despite Mtb55 containing canonical primary anchor residues.

Screening of pathogen- and self-derived peptides predicted to bind HLA-E

A selection of previously described HLA-E-restricted peptides derived from a range of self-proteins or pathogens were screened in the ELISA assay [10,12–15,29–32] (Fig. 6). A range of relative binding strengths was observed for these peptides including a Heat Shock Protein-derived peptide (Hsp5, GMKFDRGYI), a Fam49B peptide (FYAEATPML), and a Hep C Core protein-derived 10mer (YLLPRRGPRRL) that generated average absorbance readings only marginally above that of the peptide-free control (Fig. 6A). Further, an Influenza Matrix peptide (ILGFVFTLT) previously reported to bind HLA-E yielded ELISA signals below that of the negative control. However, three peptides in this panel, including the EBV-derived BZLF1 (SQAPLPCVL), the Heat Shock

Protein-derived Hsp4 (QMRPVSRVL) and the Salmonella-derived GroEL (KMLRGVNVL), produced ELISA signals greater than double the background signal. The Hsp4 and BZLF1 peptides generated particularly strong signals that respectively comprised 45 and 41% of the VL9 positive control signal following background subtraction (Supporting Information Table S2). Although both GroEL and Hsp4 peptides contained the canonical primary anchor residues, position 2 Met and position 9 Leu, the BZLF1 peptide contained a polar Gln at position 2 in addition to a Cys in place of the canonical Val or Leu at the secondary anchor position 7. Further, despite the presence of canonical primary anchor residues, the Hsp4 peptide contains a charged Arg at both positions 3 and 7 in place of the preferred smaller canonical Ala at secondary anchor position 3 and the canonical hydrophobic Val or Leu at secondary anchor position 7 in VL9 peptides.

Only one peptide in this panel, the Hepatitis C virus Core protein-derived peptide (YLLPRRGPRRL), comprised a decamer sequence [12]. However, this 10mer contains an internal nonameric sequence (LLPRRGPRRL) that aligns more optimally to the canonical binding motif of HLA-E, with hydrophobic residues at positions 2 and 9. We thus compared binding of the LLPRRGPRRL nonamer to the original decamer peptide and found that the average absorbance reading for the nonamer was more than double that of the original 10mer indicating that this shorter peptide is perhaps the optimal binder (Fig. 6B).

Screening of high affinity HLA-E peptides with anchor residue mutations

To investigate HLA-E B pocket tolerability, VL9 peptide variants with substitutions at position 2 were synthesized and screened in the optimized peptide-exchange binding assay (Fig. 7). First, a small panel based on the HLA-B7-derived leader peptide, VMAPRTVLL, was tested. Three of the four peptides in this panel, including a positively charged Lys and a polar Gln, demonstrated strong HLA-E binding, and generated average absorbance readings with the greatest degree of statistical significance (Fig. 7A). A second panel of position 2 anchor residue variants based on an alternative VL9 peptide (VMAPRTLLL) derived from the HLA-A1 leader sequence was also screened (Fig. 7B). All seven peptides in this panel demonstrated significant binding to HLA-E, includ-

Figure 2. Optimization of UV exposure duration in the peptide exchange reaction. (A) Average absorbance readings from three sandwich ELISAs where the peptide exchange reaction was sampled at 0, 1, and 2 h of UV exposure. The Y-axis denotes average absorbance readings at 450 nm and the X-axis denotes duration of UV exposure. Peptide to background signal ratios are denoted above error bars. (B) Average absorbance readings from three sandwich ELISAs where the peptide exchange reaction was sampled at 2, 3, and 4 h of UV exposure. The Y-axis denotes average absorbance readings at 450 nm and the X-axis denotes duration of UV exposure. Peptide to background signal ratios are denoted above error bars. (C) Average absorbance readings from six sandwich ELISAs where the peptide exchange reaction was sampled at 0, 2, 3, 4, 5, and 24 h in the absence of UV exposure. The Y-axis denotes average absorbance readings at 450 nm and the X-axis denotes duration of the peptide exchange reaction at 4°C. Peptide to background signal ratios are denoted above error bars. Shared Figure legend colorings are denoted with individual peptide IDs and sequences listed. Peptide ID, sequence, origin, and corresponding references are detailed in Supplementary Table S1, A (iv). Positive control peptide VL9 (HLA-B7-derived leader sequence peptide VMAPRTVLL) shown in dark blue with peptide free background (No rescue) in grey. Three biological repeats, namely, three individual peptide exchange reactions per test peptide were carried out simultaneously ($n = 3$), with two technical replicates sampled from the same peptide exchange reaction performed for each biological repeat (technical replica = 2). Stars above error bars reflect degree of significance in peptide binding by two-tailed t-tests (no star, $p > 0.05$, * $p \leq 0.05$, ** $p \leq 0.01$, *** $p \leq 0.001$, **** $p \leq 0.0001$). Error bars depicting SD of biological repeats are shown.

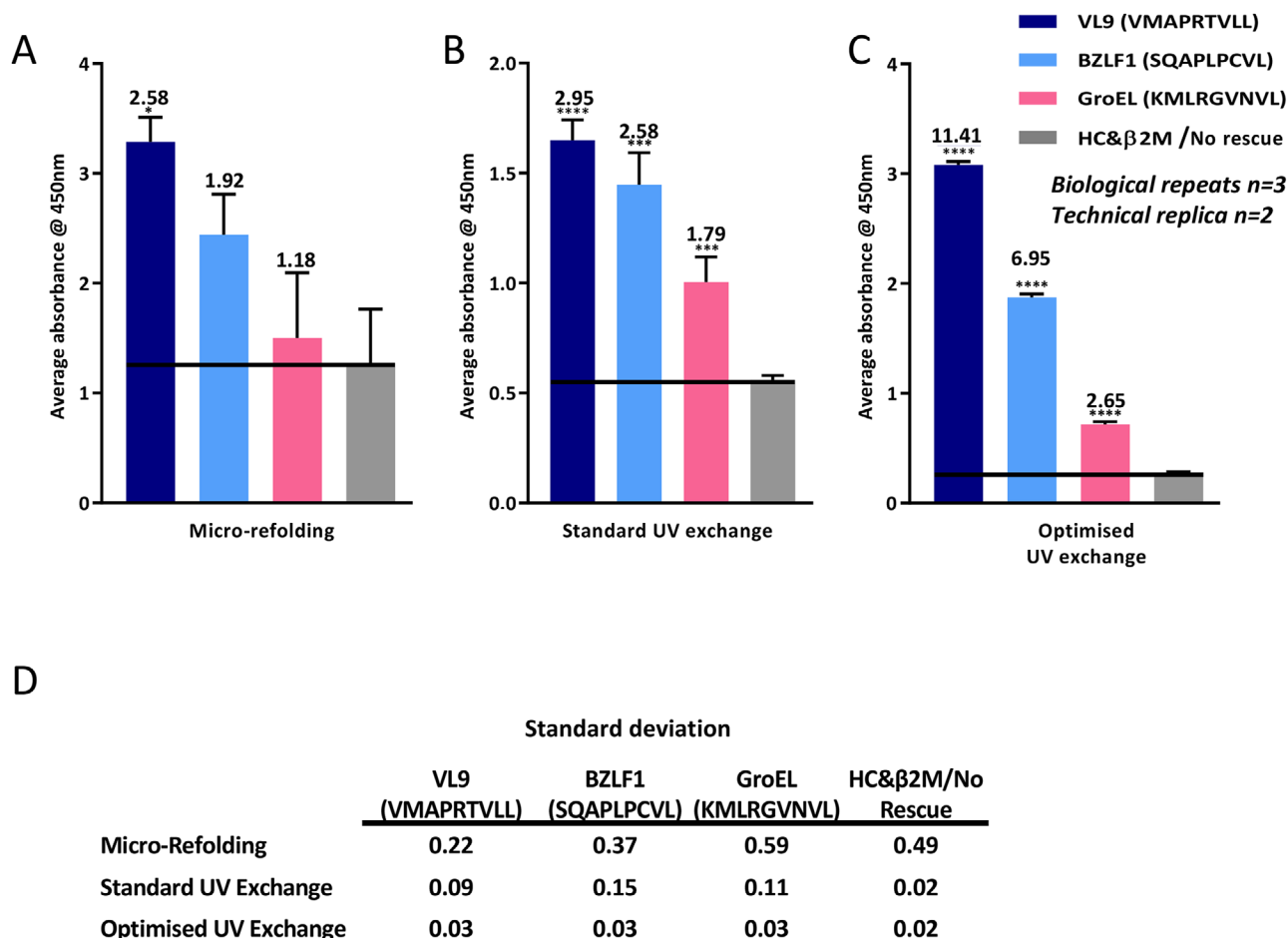


Figure 3. Comparison of micro-refold versus UV exchange peptide binding assay approaches. Average absorbance readings for 2 HLA-E-binding pathogen-derived peptides sampled in the previously published micro-refolding peptide binding affinity assay (A), the initial (standard) UV-exchange peptide binding affinity approach (B), and the optimized non-UV-exchange peptide binding assay approach (C). The Y-axis denotes average absorbance readings at 450 nm and the X-axis denotes test peptides, which are color-coded according to the shared Figure legend. Peptide to background ratios are indicated above each bar, with peptide ID and sequences denoted. The sequence, origin and corresponding references are detailed in Supporting Information Table S1, (C) The positive control peptide VL9 (HLA-B7-derived leader sequence peptide, VMAPRTVLL) is shown in dark blue. Peptide free negative backgrounds are noted in grey; for the micro-refold approach this consisted of HLA-E heavy chain and β2M only (HC and β2M) whereas the UV/non-UV peptide exchange approach negative control comprised previously refolded HLA-E complexes with no added rescue peptide in the exchange reaction (No Rescue). Three biological repeats, namely, three individual peptide exchange reactions per test peptide were carried out simultaneously ($n = 3$), with two technical replicates sampled from the same peptide exchange reaction performed for each biological repeat (technical replica = 2). Stars above error bars reflect degree of significance in peptide binding by two-tailed t-tests (no star, $p > 0.05$, $p \leq 0.05$, $**p \leq 0.01$, $***p \leq 0.001$, $****p \leq 0.0001$). Error bars depicting the SD between biological repeats are shown. (D) Table of SD for the micro-refold and the initial UV and optimized non-UV peptide exchange binding assay approaches.

ing Glu at position 2. A polar position 2 Gln yielded the strongest binding signals for both the HLA-B7 and HLA-A1 leader peptides demonstrating a degree of consistency in hierarchies of relative binding affinity between VL9 peptide variants.

Mtb44 peptide variants with a range of non-canonical primary anchor residues at positions 2 and 9 were also screened (Fig. 7C). The inclusion of charged anchor residues such as Glu or Lys at positions 2 or 9 greatly reduced binding of Mtb44 peptide variants to HLA-E, although Lys at position 2 did yield significant HLA-E binding. In addition to WT Mtb44, three variants demonstrated HLA-E binding with the greatest degree of statistical significance in the peptide-exchange assay, including those with position 2 or 9 Phe and position 2 Gln substitutions.

ELISA-based HLA-E peptide binding sequence motif

ELISA signals for peptides screened in the peptide exchange assay were normalized via background (no-peptide rescue) subtraction and subsequently expressed as percentages of the positive control VL9 peptide signal enabling the establishment of an inter-assay hierarchy of peptide binding to HLA-E presented as a heat map in Fig. 8A. Peptides were ranked in order of relative binding strength to HLA-E according to ELISA data and subdivided into 11 categories from those that generated signals below background levels to those that generated signals ranging from 70 to 100% of the positive control signal following background subtraction (Supporting Information Table S2). A Seq2Logo HLA-E sequence

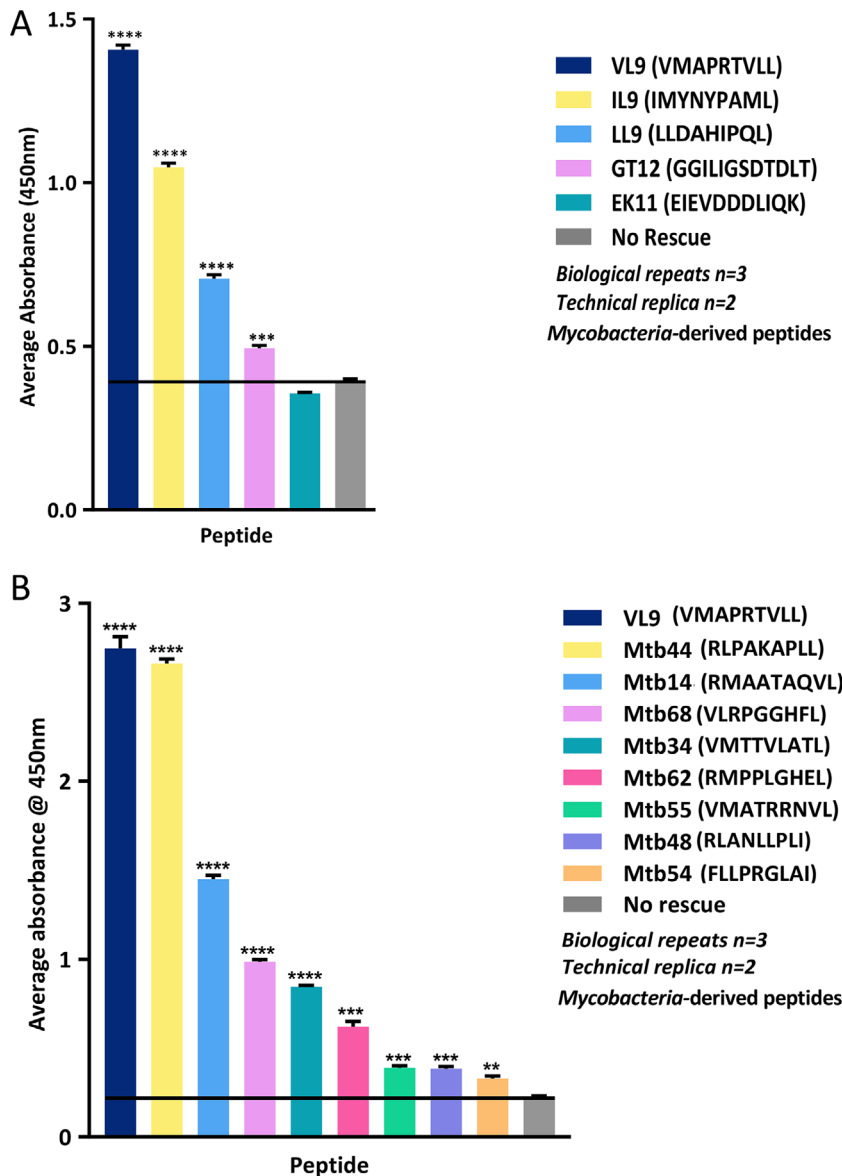


Figure 5. Screening of *Mycobacteria*-derived peptides in the HLA-E peptide exchange ELISA assay. (A) Average absorbance readings from the peptide exchange binding assay for Mtb-derived peptides eluted from infected cells. Peptide sequences are denoted in the corresponding Figure legend. Peptide ID, sequence, origin and corresponding references are detailed in Supporting Information Table S1, B (i). (B) Average absorbance readings from the peptide exchange binding assay for Mtb-derived peptides previously predicted to bind HLA-E. Peptide sequences are denoted in the corresponding Figure legend. Peptide ID, sequence, origin and corresponding references are detailed in Supporting Information Table S1, B (ii). Average absorbance readings at 450 nm for plots in A and B are displayed on the Y-axis. Positive control peptide VL9 (HLA-B7-derived leader sequence peptide VMAPRTVLL) shown in dark blue with peptide free background (No rescue) in grey. Three biological repeats, namely, three individual peptide exchange reactions per test peptide were carried out simultaneously ($n = 3$), with two technical replicas sampled from the same peptide exchange reaction performed for each biological repeat (technical replica = 2). Stars above error bars reflect degree of significance in peptide binding by two-tailed t-tests (no star, $p > 0.05$, * $p \leq 0.05$, ** $p \leq 0.01$, *** $p \leq 0.001$, **** $p \leq 0.0001$). Error bars depicting the SEM are shown.

infection and Cytomegalovirus-vectored SIV vaccination, respectively, suggests an unanticipated role for HLA-E in the context of T cell immunity. This previously undiscovered role is exciting and offers potential for “universal” HIV vaccine development. Central to this is a requirement to develop sensitive tools to re-appraise the peptide binding ligandome of HLA-E. Consequently, we have designed and optimized a highly sensitive peptide exchange ELISA-based assay enabling the relative quantification of peptide binding to HLA-E. Comparative assays demonstrated this new peptide exchange technique offers superior sensitivity and reliability relative to the previously published HLA-E peptide binding ELISA [7,20].

Regarding assay optimization, the identification of peptide exchange independent of photo-illumination raises the question of whether the photo-labile VL9-based peptide (VMAPIJTLVL) is cleaved by lower wavelengths in the visible spectrum or by background UV radiation present in the lab. Alternatively, it is

possible that full length, nonameric UV-labile peptide dissociates from the HLA-E binding groove over time in the absence of rescue peptide, irrespective of exposure to electromagnetic radiation. We previously showed, via blue native gel analysis of HLA-E, that a molar excess of lower affinity peptide (RL9HIV) can facilitate peptide exchange with a pre-bound higher affinity VL9 peptide [20]. This demonstrates that peptide exchange from a higher to lower affinity peptide ligand is possible for HLA-E in the absence of a photo-cleavable peptide or UV irradiation when the lower affinity peptide is in molar excess. Further, the introduction of an unnatural beta amino acid at position 5 of the UV-labile VL9 peptide results in conformational changes to the peptide main chain that can in turn impact binding affinity [23]. Therefore the modified VL9 peptide might have an even greater propensity for dissociation and peptide exchange relative to WT VL9.

Despite optimization strategies improving both reliability and sensitivity of the peptide exchange ELISA assay, some techni-

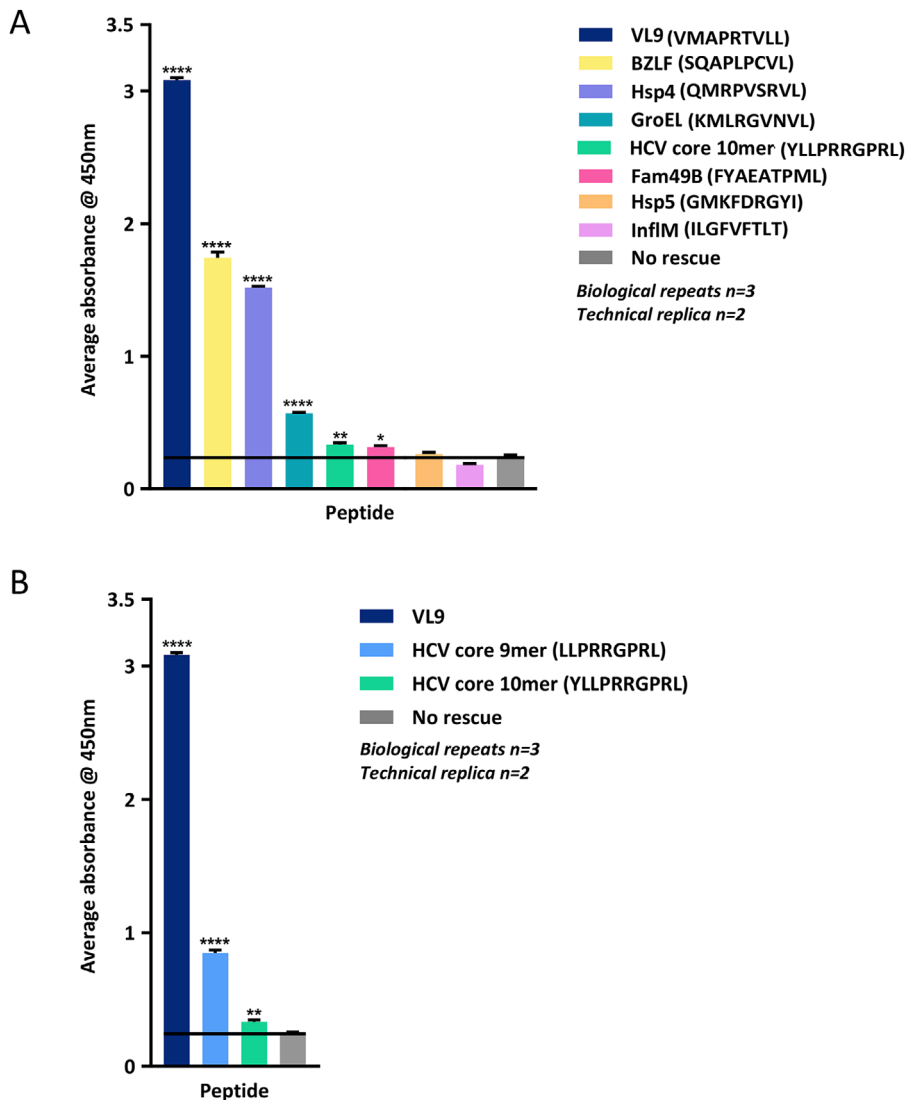
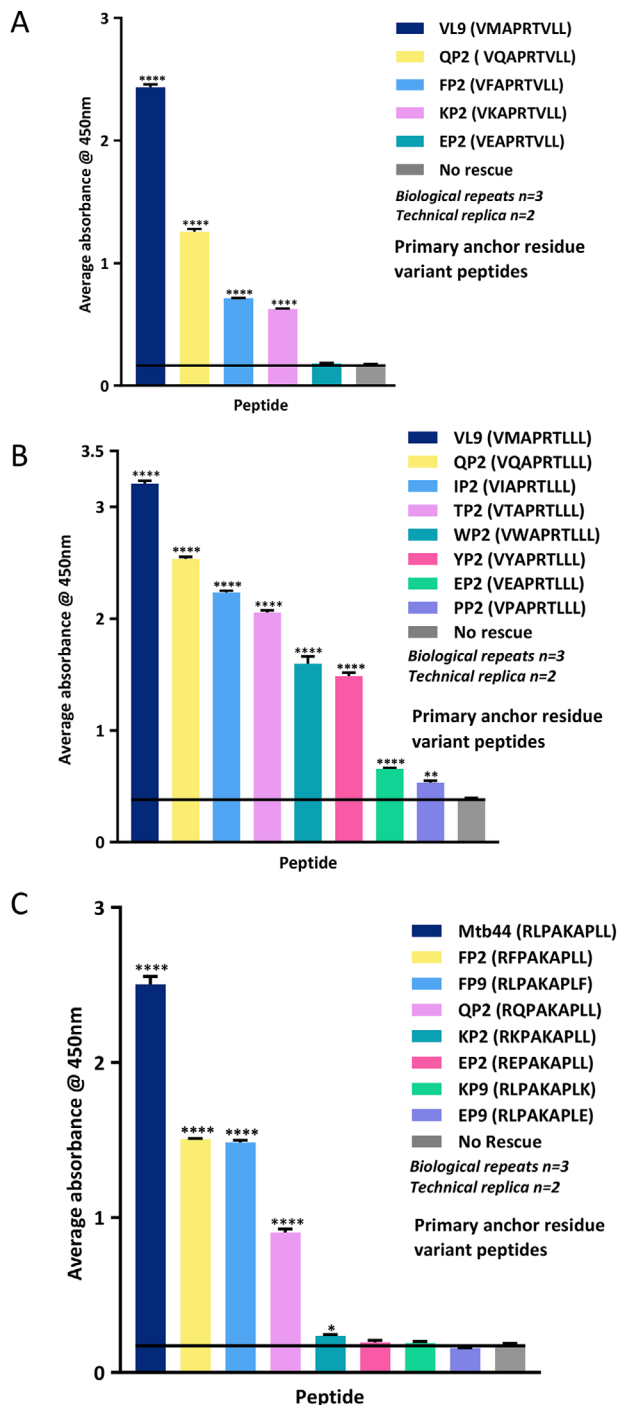


Figure 6. Screening of self- and pathogen-derived peptides previously predicted to bind HLA-E in the peptide exchange ELISA assay. (A) Average absorbance readings for pathogen- and self-derived HLA-E binding peptides screened in the peptide exchange ELISA-based assay for HLA-E binding capacity. Peptide sequences are denoted in the corresponding Figure legend. Peptide ID, sequence, origin and corresponding references are detailed in Supporting Information Table S1C (i). (B) Peptide exchange ELISA-based assay comparison of the previously described Hepatitis C virus Core protein-derived decamer peptide and an internal nonameric predicted binding variant that adheres more optimally to the HLA-E binding motif and lacks the N-terminal Tyr of the parental peptide. Average absorbance readings at 450nm are displayed on the Y-axis for A and B. Positive control peptide VL9 (HLA-B7-derived leader sequence peptide VMAPRTVLL) shown in dark blue with peptide free background (No rescue) in grey. Three biological repeats, namely, three individual peptide exchange reactions per test peptide were carried out simultaneously ($n = 3$), with two technical replicas sampled from the same peptide exchange reaction performed for each biological repeat (technical replica = 2). Stars above error bars reflect degree of significance in peptide binding by two-tailed t-tests (no star, $p > 0.05$, * $p \leq 0.05$, ** $p \leq 0.01$, *** $p \leq 0.001$, **** $p \leq 0.0001$). Error bars depicting the SEM are shown.

cal challenges remain. First, inter-assay variation may be introduced due to stability differences in macro-refolded HLA-E- β 2M-VMAPJTLVL complexes. Since the UV-labile VL9 ligand appears to dissociate from pre-refolded HLA-E complexes in the absence of UV-illumination, the precise timings of size exclusion chromatography, purified protein concentration, and subsequent freezing methods could influence the degree of peptide dissociation prior to the peptide exchange reaction, and subsequently impact ELISA data. To account for such inter-assay variation, we normalized average absorbance readings of test peptides by subtracting the background signal and subsequently expressing binding signals as percentages of VL9 binding before generating an overall inter-assay hierarchy of peptide binding to HLA-E. Additionally, VL9 positive control peptides generate much higher average absorbance readings than the majority of screened peptides and these positive control signals remain unaffected when the VL9 peptide concentration is titrated from 100 to below 10 μ M (Supporting Information Fig. S1). This, coupled with increased assay sensitivity, renders sample spacing on ELISA plates a crucial factor

to consider to avoid cross-contamination. We observed that ELISA wells containing the VL9 positive control must be separated by at least two wells in each direction or ideally be placed on a separate plate to avoid this issue (data not shown). This also extends to medium binding peptides that generate signals over 10% of the VL9 positive control following background subtraction—such peptides must also be separated by multiple wells from lower affinity, non-binding peptides or negative controls to eliminate false positive results.

The optimized peptide exchange ELISA assay reliably demonstrated HLA-E binding to a range of pathogen- and self-derived peptides with sequences that deviate from the canonical VL9 peptide. Such results support previous findings that in certain physiological contexts the HLA-E peptide binding repertoire might not be limited to MHC class I-derived leader peptides [17]. Despite this, our results are consistent with the original characterization of the HLA-E peptidome, in which a strong preference for VL9 peptides was established [6,1]. Of all the screened peptides, only one (Mtb44, RLPKAPLL) exhibited comparable binding signals



to the positive VL9 peptide—the Mtb44 signal represented 97% of VL9 following background subtraction (Supporting Information Table S2). The majority of peptides tested exhibited exceptionally low binding signals many of which were indistinguishable from the negative control peptide-free background. However, a small selection of pathogen- or self-derived non-VL9 peptides demonstrated reliable, statistically significant binding to HLA-E and generated average absorbance readings above 10% of the VL9 con-

trol following background subtraction (Supporting Information Table S2). The majority of these >10% of VL9 “medium” strength HLA-E-binders contained the canonical primary anchor residues at positions 2 (Met) and 9 (Leu). However, BZLF1 (SQAPLPCVL) contains a polar Gln at position 2 in place of the hydrophobic Met and the NetMHC-HIV-7 (VIWGKTPKF) peptide contains a larger aromatic Phe at position 9. Our previous blue native gel analysis established that peptides, such as RL9HIV (RMYSPTSIL), within the medium affinity category that reliably generate the greatest peptide to background ratios other than VL9 or Mtb44 (RLPAKAPLL) in the ELISA assay, produce multiple gel bands on blue native gel analysis, indicative of heterogeneous protein populations [20]. Thus, HLA-E-restricted peptides in the medium affinity category established in this study are unlikely to support formation of homogeneous fully folded HLA-E forms. However, we were previously able to obtain crystal structures of HLA-E bound to medium affinity peptides, including RL9HIV (RMYSPTSIL), indicating that a subpopulation of fully folded material was present and incorporated into the crystal lattice [20]. Previously obtained peptide-bound structures of HLA-E and their corresponding ELISA rankings are listed in Supporting Information Table S3. Although such structures were obtained for HLA-E binding peptides that generated ELISA signals between 31.3 and 96.5% of the VL9 positive control following buffer subtraction, crystals could not be grown for lower binding peptides likely owing to increased complex instability inhibiting lattice formation. Also, crystals were not obtained for the BZLF EBV-derived peptide (SQAPLPCVL) despite its ELISA ranking (40.7% of VL9) falling within range of other crystallizable peptides.

To further probe the tolerability of the primary anchor B and F pockets of the HLA-E binding groove, we synthesized VL9- and Mtb44-based peptide variants and screened these primary anchor mutant peptides in the peptide exchange ELISA assay (Fig. 7).

Figure 7. Peptide exchange ELISA binding assay screening of VL9 and Mtb44 position 2 and 9 primary anchor residue variants. (A) Average absorbance readings from the peptide-exchange sandwich-ELISA-based binding assay for a selection of VL9 position 2 variant peptides. The positive control VL9 peptide (VMAPRTVLL) is shown in dark blue with the peptide-free background (No rescue) in grey. Peptide ID, sequence, length and corresponding references are detailed in Supporting Information Table S1D (i). (B) Average absorbance readings from the peptide-exchange sandwich-ELISA-based binding assay are denoted on the Y-axis for a selection of VL9 position 2 variant peptides based on the sequence, VMAPRTLIL. Peptide details are listed in Supporting Information Table S1D (i). (C) Average absorbance readings from the peptide-exchange sandwich-ELISA-based binding assay for a collection of Mtb44 primary anchor residue variant peptides with a range of alternative hydrophobic, polar or charged residues in place of the canonical primary anchor residues. The positive control WT Mtb44 peptide (RLPAKAPLL) is shown in dark blue with the peptide-free background (No rescue) in grey. Average absorbance readings at 450nm are displayed on the Y-axis for plots in (A–C). Peptide details and corresponding references are denoted in Supporting Information Table S1D (ii). Three biological repeats, namely, three individual peptide exchange reactions per test peptide were carried out simultaneously (n=3), with two technical replicates sampled from the same peptide exchange reaction performed for each biological repeat (technical replica = 2). Stars above error bars reflect degree of significance in peptide binding by two-tailed t-tests (no star, $p > 0.05$, * $p \leq 0.05$, ** $p \leq 0.01$, *** $p \leq 0.001$, **** $p \leq 0.0001$). Error bars depicting the SEM are shown.

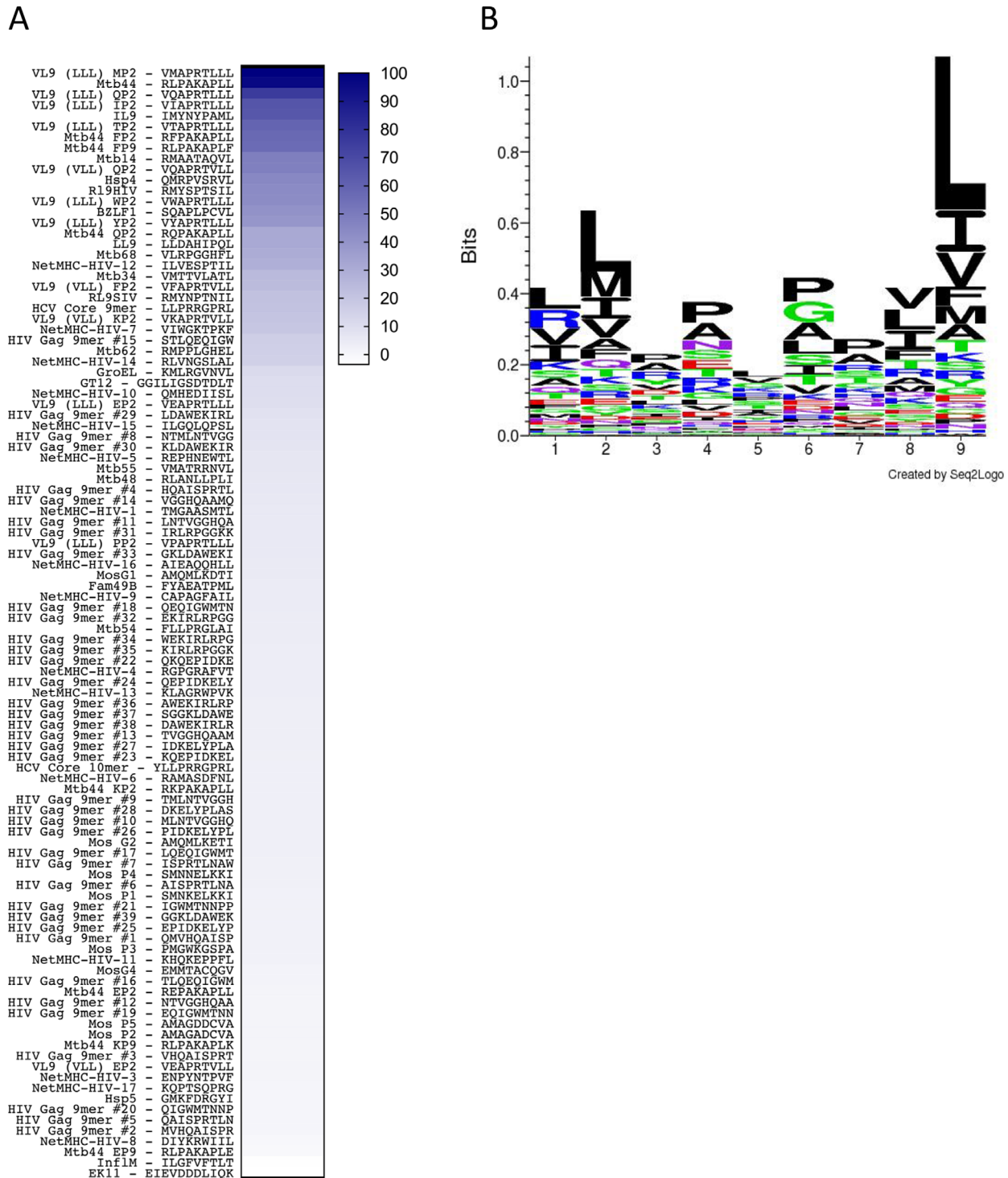


Figure 8. Hierarchy of peptide binding to HLA-E and Seq2Logo peptide binding motif. (A) A heat map depicting peptides screened in the peptide exchange ELISA-assay in descending order of relative binding strength to HLA-E. Screened peptides were ranked in order of binding strength to HLA-E by expressing each peptide signal as a percentage of the positive control VL9 signal following background subtraction to normalise for inter-assay variation. Each peptide is listed in Supporting Information Table S1 along with its sequence, ID and corresponding percentage of VL9 signal after background subtraction. (B) A Seq2Logo HLA-E peptide sequence motif based on statistically significant nonameric peptides that generated peptide exchange ELISA-based assay signals within 20–100% of the positive control VL9 signal after background subtraction. Primary anchor residue variant peptides based on either VL9 or Mtb44 peptide backgrounds were excluded from analysis to remove bias from overrepresented residues at remaining non-mutated positions. The Y-axis denotes information in bits with peptide position plotted on the X-axis. Letters represent amino acids with font size indicating residue frequency. The length of residue stacks indicates the degree of conservation among inputted sequences at that position with small letter stack lengths reflecting increased residue variability.

A number of Mtb44 and VL9 variant peptides supported HLA-E binding despite the presence of non-canonical primary anchor residues such as a Thr, Ile, Gln, Tyr, Trp, Phe, or positively charged Lys at position 2 of VL9. Notably, the hierarchy of relative binding of position 2 anchor residue mutations differed on the Mtb44 and VL9 peptide panel backgrounds, indicating other positions along these nonamers operate synergistically with position 2 substitutions to determine overall peptide binding affinity. For example, position 2 Lys generated low ELISA signals when substituted into the Mtb44 peptide backbone but yielded stronger binding when inserted into the VL9 nonamer. Furthermore, Gln at position 2 of the VL9 peptide yielded stronger binding to HLA-E compared to the position 2 Phe VL9 peptide variant. However, this trend was reversed for Mtb44 with the position 2 Phe variant demonstrating stronger binding to HLA-E, above that of the position 2 Gln variant. The presence of non-canonical primary anchor residues in HLA-E binding peptides does not however necessarily indicate broad receptivity of respective pockets. Structural evidence would be required to elucidate whether non-canonical primary anchor side chains occupy their corresponding pockets, or whether these peptides adopt alternative binding conformations.

Early experiments delineating the HLA-E binding motif analyzed acid eluted peptide from in vitro refolded HLA-E with VL9 anchor residue variant peptide libraries via mass spectrometry [34]. However, the HLA-E binding groove's capacity to accommodate suboptimal peptides and the sequence identity of potential non-VL9 HLA-E-binding peptides was not fully elucidated. For example, the sensitivity of peptide elution from in vitro refolded HLA-E would have been compromised by the co-presence of an excess of near optimal VL9 variant peptide in the pool—such as those with position 2 Met to Leu or Ile substitutions that were shown to only marginally reduce binding affinity to HLA-E [34]. Peptides with lower binding affinities would likely have been out-competed in these settings and thus remain undetected. By contrast, the peptide exchange ELISA assay presented here affords superior sensitivity as the binding capacity of suboptimal HLA-E binding peptides is tested in the absence of competition from higher affinity peptide. Although previous mass spectrometry studies identified an extended hydrophobic primary anchor motif for HLA-E that included residues such as Ile and Leu in addition to Met at position 2, our motif analysis builds on previous work. The HLA-E peptide binding motif based on screens presented here demonstrates that additional hydrophobic residues such as Val, Ala, and Phe can be tolerated at both primary anchor positions in addition to a polar Gln at position 2 (Fig. 8B). This extended motif is supported by our previously published structures of HLA-E in complex with Mtb44 (RLPKAPLL) primary anchor variant peptides containing a Phe at position 2, Phe at position 9, and Gln at position 2 [20]. All substituted primary anchor side chains were accommodated by their corresponding primary B and F pockets and superposed to the WT anchor side chains demonstrating increased primary pocket tolerability. Beyond this, our ELISA-based HLA-E sequence motif also highlighted the importance of a central Pro at positions 3, 4, 6, or 7. Interestingly, peptides that satisfied the primary anchor motif demonstrated a large range of binding strength for HLA-E in

the peptide exchange ELISA assay thus illustrating that the presence of particular hydrophobic residues at positions 2 and 9 is not sufficient for optimal HLA-E binding. However, 10 of the 12 non-VL9 pathogen- or self-derived peptides (excluding Mtb44 and VL9 primary anchor variant peptides) that generated signals >20% of VL9 following background subtraction contained a Pro at a central position in the peptide, in addition to tolerated primary anchors. For example, Mtb44 (RLPAKAPLL), the strongest binding peptide tested, contains a Pro at both positions 3 and 7. Further, two peptides that bind >20% of VL9, RL9HIV and RL9SIV, contain a Pro at the largely unrestricted position 5 as opposed to position 3, 4, 6, or 7, as indicated by the novel HLA-E sequence motif. However, the alternative peptide backbone conformation observed in the structure of RL9HIV-bound HLA-E causes the position 5 Pro side chain to align to position 6 of VL9 peptides, project toward the groove floor and thereby act as a compensatory position 6 secondary anchor residue [35]. In this way, the Pro at position 5 of RL9HIV and RL9SIV peptides is equivalent to position 6 in other HLA-E binding peptides that adopt the classical kinked peptide configuration and contain a largely solvent exposed position 5 that projects away from the binding groove (such as Mtb44, RLPKAPLL) [35]. Thus, the RL9HIV and RL9SIV peptides functionally adhere to the Seq2Logo motif. By contrast, the vast majority of test peptides which satisfy the primary anchor motif and generated signals <5% of VL9 following background subtraction, including NetMHC-HIV-8 (DIYKRWIIL), Hsp5 (GMKFDRGYI), HIV Gag 9mer #16 (TLQE-QIGWM), MosG4 (EMMTACQGV), MosP1 (SMNKLKKI), MosP4 (SMNNELKKI), MosG2 (AMQMLKETI), HIV Gag 9mer #26 (PID-KELYPL), NetMHC-HIV-6 (RAMASDFNL), HIV Gag 9mer #13 (TVGGHQAAM), MosG1 (AMQMLKDTI), and NetMHC-HIV-16 (AIEAQQHLL), lacked a centrally-positioned Pro illustrating the importance of this additional component of the optimal HLA-E peptide sequence motif.

A Met to Thr substitution present at position 2 in a subset of HLA-B27 (VTAPRTLII) and HLA-B15 (VTAPRTVLL) leader peptides has previously been shown to reduce HLA-E cell surface expression due to decreased peptide affinity and complex stability [2,4]. Thus, it could be predicted that other pathogen- or self-derived peptides with lower peptide exchange ELISA assay rankings to that of VL9 position 2 Thr (Supporting Information Table S2), might also exhibit compromised cell surface expression and reduced representation in the steady-state HLA-E-presented repertoire. However, the primary contexts in which HLA-E- or Mamu-E-restricted epitopes have been identified involve deregulated MHC class I trafficking pathways [17,18,21]. It is possible that perturbations in the supply of MHC class I-derived VL9 peptides in addition to alternative trafficking due to Mtb- or CMV vector-driven immune evasion mechanisms, give rise to lower affinity, non-canonical peptides in the cell surface-presented HLA-E ligandome.

Intriguingly a number of key epitopes against which HLA-E-restricted CD8⁺ T cell responses have previously been identified did not exhibit definitive HLA-E binding in this assay. For example, the Mtb-derived EK11 (EIEVDDDLIQK), which comprises residues 19–29 of the conserved hypothetical protein Rv0634A, demonstrated an immunodominant profile with HLA-E-restricted

responses detected in 81% of tested donors with active or latent Mtb infection [21]. However, in the peptide exchange ELISA assay EK11 generated absorbance readings below the “no-rescue” peptide-free background signal, and produced the lowest signal of any peptide tested (Supporting Information Table S2). Further, a Fam49B-derived peptide (FYAEATPML) previously shown to elicit Qa-1-restricted CD8⁺ T cell responses, also demonstrated exceptionally low signals below 5% of the VL9 positive control (Fig. 6A; Supporting Information Table S2) [14]. Such results are consistent with previous micro-refolding ELISA and single chain trimer transfection data that indicate the 11 optimal SIV epitopes in RhCMV 68-1 vector-based vaccine studies also bind HLA-E with dramatically lower relative affinity than the positive control VL9 peptide, with some generating signals only marginally above background [17]. Surprisingly, these epitopes appear to play a protective role despite not supporting HLA-E complex stability in this assay system. It therefore appears that HLA-E peptide binding affinity may not always correlate with the strength of the CD8⁺ T cell response elicited and that perhaps two modes of HLA-E-restricted CD8⁺ T cell recognition exist; the first of which comprises conventional recognition of medium strength HLA-E-restricted peptides and the second of which involves exceptionally low affinity or apparent non-binders. Alternatively, the conditions of our in vitro assay may not adequately reflect the intracellular environments that support MHC-E peptide loading in RhCMV 68-1 vaccinated or Mtb-infected cells. Equally, it is possible that the conventional mode of peptide binding might not apply in these settings but instead a currently unknown mechanism could facilitate suboptimal peptide presentation or stabilize low affinity peptide binding to MHC-E. Abacavir, an anti-retroviral nucleoside analogue reverse transcriptase inhibitor used to treat HIV-infected individuals, was structurally demonstrated to specifically sit in the C, E, and F pockets of HLA-B*57:01, in turn altering the presented peptide repertoire and resulting in self-reactivity [36]. It is possible that, analogous to this drug-modified repertoire, pocket stabilizing interactions with an unidentified co-factor might exclusively occur in contexts such as RhCMV 68-1-SIV vaccination or Mtb infection, allowing HLA-E stabilization and altering the peptide binding groove preferences to facilitate presentation of low affinity peptides.

In summary, the highly sensitive peptide exchange ELISA-based assay presented here can reliably establish the relative HLA-E binding capacity of test peptides. Considering HLA-E-, Qa-1-, and Mamu-E-restricted CD8⁺ T cell responses have been identified in various contexts of vaccination, infection, and autoimmune disease, this assay provides a useful tool to determine binding strength of putative HLA-E-restricted epitopes. Further, this assay can be used to screen algorithmically identified peptides predicted to support HLA-E complex stability, thus potentially enabling the identification of novel HLA-E-restricted peptides that could subsequently be targeted in therapeutic or vaccine settings. In future, it will be important to determine the underlying basis of MHC-E-restricted CD8⁺ T cell recognition and resolve how remarkably low affinity or apparent “non-binding” peptides elicit HLA-E-, Qa-1- or Mamu-E-restricted CD8⁺ T cell responses in vivo [17].

Materials and methods

Peptide synthesis

Synthetic peptides were generated by Fmoc (9-fluorenylmethoxy carbonyl) chemistry to a purity of >85% by Genscript USA. All peptides were provided as lyophilized powder, reconstituted in DMSO to a concentration of 200 mM, and stored at –80°C. A UV photolabile version of the HLA-B leader sequence peptide, VMAPRTLVL, incorporating a UV-sensitive 3-amino-3-(2-nitrophenyl)-propionic acid residue (J residue) substitution at position 5, VMAPJTLVL was synthesized by Dris Elatmioui at LUMC, The Netherlands. The UV-sensitive peptide (termed 7MT2) was stored as lyophilized powder, and reconstituted as required.

HLA-E protein refolding and purification

β2-Microglobulin in Urea-Mes, at a final concentration of 2 μM, was refolded at 4°C for 30 min in a macro-refolding buffer prepared in MiliQ water containing 100 mM Tris, pH 8.0, 400 mM L-arginine monohydrochloride, 2 mM EDTA, 5 mM reduced glutathione, and 0.5 mM oxidized Glutathione. The UV-sensitive peptide 7MT2 was subsequently added to the β2M refold to achieve a peptide concentration of 30 μM. HLA-E*01:03 heavy chain was subsequently pulsed into the refolding buffer until a final concentration of 1 μM was reached. Following incubation for 72 h at 4°C, HLA-E refolds were filtered through 1.0 μm cellular nitrate membranes to remove aggregates prior to concentration by the VivaFlow 50R system with a 10 kDa molecular weight cut-off (Sartorius) and subsequent concentration in 10 kDa cut-off VivaSpin Turbo Ultrafiltration centrifugal devices (Sartorius). Samples were then separated according to size into 20 mM Tris pH8, 100 mM NaCl by fast protein liquid chromatography (FPLC) on an AKTA Start System using a Superdex S75 16/60 column. Elution profiles were visualized by UV absorbance at 280 mAU, enabling differentiation of correctly refolded HLA-E-β2M-peptide complexes from smaller non-associated β2M and larger misfolded aggregates. FPLC-eluted protein peak fractions were combined and concentrated to 3 mg/mL using 10 kDa cut-off VivaSpin Turbo Ultrafiltration centrifugal devices prior to use in the HLA-E peptide exchange ELISA-based assay. One microliter aliquots were analyzed by non-reducing SDS-PAGE electrophoresis on NuPAGE™ 12% Bis-Tris protein gels (ThermoFisher Scientific) to confirm the presence of non-aggregated HLA-E heavy chain and β2m.

HLA-E peptide exchange reaction

The optimization of this technique is detailed in the Results section. Following optimization, 3 μg of purified HLA-E previously refolded with the UV sensitive peptide 7MT2 was incubated in the presence of 100 μM “exchange” peptide in polypropylene V-shaped 96-well plates (Greiner Bio-One) for 5 h on ice. The final volume of each well was adjusted to 125 μL by adding

exchange buffer comprising 100 mM Tris pH8.0, 400 mM L-arginine monohydrochloride, 2 mM EDTA, 5 mM reduced glutathione, and 0.5 mM oxidized Glutathione, prepared in MiliQ water.

Sandwich ELISA

The 96-well ELISA plates (Life Technologies) were coated with the anti-human HLA-E monoclonal capture antibody, 3D12 (BioLegend), diluted to 10 µg/mL in freshly prepared ELISA Coating Buffer (BioLegend) and incubated for 12 h at 4°C. Wells were washed three times in 200 µL PBS, and subsequently incubated in 300 µL of 2% IgG-free BSA (Sigma Aldrich) for 2 h at room temperature to block unoccupied surfaces on the ELISA plate wells to prevent non-specific protein binding. Following plate blocking, plates were washed five times with 200 µL freshly prepared 0.05% Tween-based ELISA Wash Buffer (BioLegend) and a final time in 200 µL PBS (all subsequent plate washing was carried out in an identical manner). Fifty microliters of the HLA-E reaction mixture from either micro-scale refolding or UV/non-UV-induced peptide exchange, diluted 1:100 in 2% BSA, was added to each well of the ELISA plate and left to incubate for 1 h at room temperature. Following protein incubation and subsequent plate washing, 50 µL of polyclonal anti-human β2M HRP-conjugated IgG detection antibody raised in rabbits (ThermoFisher Scientific), diluted 1:2500 in 2% BSA (0.2 µg/mL), was added to each well to ensure detection of β2M-associated forms of HLA-E only. After 30 min of dark incubation at 4°C, ELISA plates were washed and 50 µL of a goat anti-rabbit HRP-conjugated IgG enhancement antibody (EnVision+ System-HRP from Agilent), diluted 1:15 in 2% BSA containing 1% mouse serum to prevent cross-reactivity, was added to each well to amplify the signal. ELISA plates were incubated for 15 min in the dark at room temperature, and following a final round of plate washing, developed in 100 µL of 3,3',5,5'-tetramethyl benzidine (TMB) substrate (BioLegend) and incubated in the dark at room temperature for a further 10 min. Finally, the reactions were terminated in 100 µL of H₂SO₄ STOP solution (BioLegend) and absorbance readings were obtained at 450 nm on a FLUOstar OMEGA plate reader. Both the peptide exchange reaction and sandwich ELISA stages of the assay are depicted in Fig. 1A. It is noteworthy that ELISA wells containing the VL9 positive control or any peptide that generates a signal above 10% of VL9 following buffer subtraction should be separated by at least two wells on the 96-well plate to avoid cross-contamination and false positive results.

Acknowledgments: This work was supported by grants from the BMGF (OPP1133649), MRC (MR/M019837/1), NIAID (5UM1AI126619-05), and the Hester Cordelia Parsons Fund, Oxford University.

Conflict of interest: The authors declare no commercial or financial conflict of interest.

References

- 1 Braud, V., Jones, E.Y. and McMichael, A., The human major histocompatibility complex class Ib molecule HLA-E binds signal sequence-derived peptides with primary anchor residues at positions 2 and 9. 1997. DOI: 10.1002/eji.1830270517.
- 2 Lee, N., Goodlett, D.R., Ishitani, A., Marquardt, H. and Geraghty, D.E., HLA-E surface expression depends on binding of TAP-dependent peptides derived from certain HLA class I signal sequences. *J. Immunol.* 1998. 160: 4951–60.
- 3 Braud, V., Calan, C.A.O., So, K., Andrea, A.D., Ogg, G.S., Lazetic, S., Young, N.T. et al., HLA-E binds to natural killer cell receptors CD94/NKG2A, B and C. 1998.
- 4 Brooks, A.G., Borrego, F., Posch, P.E., Patamawenu, A., Scorzeili, C.J., Ulbrecht, M., Weiss, E.H. et al., Specific recognition of HLA-E, but not classical, HLA class I molecules by soluble CD94/NKG2A and NK cells. *J. Immunol.* 1999. 162: 305–30513.
- 5 Llano, M., Lee, N., Navarro, F., García, P., Albar, J.P., Geraghty, D.E. and López-Botet, M., HLA-E-bound peptides influence recognition by inhibitory and triggering CD94/NKG2 receptors: preferential response to an HLA-G-derived nonamer. *Eur. J. Immunol.* 1998. 28: 2854–2863. DOI: 10.1002/(SICI)1521-4141(199809)28:09<2854::AID-IMMU2854>3.0.CO;2-W.
- 6 O'Callaghan, C.A., Tormo, J., Willcox, B.E., Braud, V.M., Jakobsen, B.K., Stuart, D.I., McMichael, A.J. et al., Structural features impose tight peptide binding specificity in the nonclassical MHC molecule HLA-E. *Mol. Cell.* 1998. 1: 531–541. DOI: 10.1016/S1097-2765(00)80053-2.
- 7 Strong, R.K., Holmes, M.A., Li, P., Braun, L., Lee, N. and Geraghty, D.E., HLA-E allelic variants: Correlating differential expression, peptide affinities, crystal structures, and thermal stabilities. *J. Biol. Chem.* 2003. 278: 5082–5090. DOI: 10.1074/jbc.M208268200.
- 8 Hoare, H.L., Sullivan, L.C., Clements, C.S., Ely, L.K., Beddoe, T., Henderson, K.N., Lin, J. et al., Subtle Changes in Peptide Conformation Profoundly Affect Recognition of the Non-Classical MHC Class I Molecule HLA-E by the CD94–NKG2 Natural Killer Cell Receptors. *J. Mol. Biol.* 2008. 377: 1297–1303. DOI: 10.1016/j.jmb.2008.01.098.
- 9 Madden, D.R., *The Three-Dimensional Structure Of Peptide-MHC Complexes.* 1995.
- 10 Lo, W-F., Woods, A.S., DeCloux, A., Cotter, R.J., Metcalf, E.S. and Soloski, M.J., Molecular mimicry mediated by MHC class Ib molecules after infection with Gram-negative pathogens. *Nat. Med.* 2000. 6: 215–218. DOI: 10.1038/72329.
- 11 Salerno-Gonçalves, R., Fernandez-Viña, M., Lewinsohn, D.M. and Szein, M.B., Identification of a Human HLA-E-Restricted CD8 + T Cell Subset in Volunteers Immunized with Salmonella enterica Serovar Typhi Strain Ty21a Typhoid Vaccine. *J. Immunol.* 2004. 173: 5852–5862. DOI: 10.4049/jimmunol.173.9.5852.
- 12 Nattermann, J., Nischalke, H.D., Hofmeister, V., Ahlenstiel, G., Zimmermann, H., Leifeld, L., Weiss, E.H. et al., The HLA-A2 restricted T cell epitope HCV core35-44 stabilizes HLA-E expression and inhibits cytolysis mediated by natural killer cells. 2005. DOI: 10.1016/S0002-9440(10)62267-5.
- 13 Ulbrecht, M., Weiss, E.H., Modrow, S., Srivastava, R. and Peterson, P.A., Interaction of HLA-E with peptides and the peptide transporter in vitro: Implications for its function in antigen presentation. 1998.

- 14 Nagarajan, N.A., Gonzalez, F. and Shastri, N., Nonclassical MHC class Ib-restricted cytotoxic T cells monitor antigen processing in the endoplasmic reticulum. *Nat. Immunol.* 2012. **13**: 579–586. DOI: 10.1038/ni.2282.
- 15 Michaëlsson, J., Teixeira de Matos, C., Achour, A., Lanier, L.L., Kärre, K. and Söderström, K., A Signal Peptide Derived from hsp60 Binds HLA-E and Interferes with CD94/NGG2A Recognition. *J. Exp. Med.* 2002. **196**: 1403–1414. DOI: 10.1084/jem.20020797.
- 16 Sensi, M., Pietra, G., Molla, A., Nicolini, G., Vegetti, C., Bersani, I., Millo, E. et al., Peptides with dual binding specificity for HLA-A2 and HLA-E are encoded by alternatively spliced isoforms of the antioxidant enzyme peroxiredoxin 5. *Int. Immunol.* 2009. **21**: 257–268. DOI: 10.1093/intimm/dxn141.
- 17 Hansen, S.G., Wu, H.L., Burwitz, B.J., Hughes, C.M., Hammond, K.B., Ventura, A.B., Reed, J.S. et al., Broadly targeted CD8+ T cell responses restricted by major histocompatibility complex E. *Science* (80-). 2016. **351**: 714–720. DOI: 10.1126/science.aac9475.
- 18 Joosten, S.A., Van Meijgaarden, K.E., Van Weeren, P.C., Kazi, F., Geluk, A., Savage, N.D.L., Drijfhout, J.W. et al., Mycobacterium tuberculosis peptides presented by HLA-E molecules are targets for human CD8+ T-cells with cytotoxic as well as regulatory activity. *PLoS Pathog.* 2010; **6**. DOI: 10.1371/journal.ppat.1000782.
- 19 Joosten, S.A., Sullivan, L.C. and Ottenhoff, T.H.M., Characteristics of HLA-E Restricted T-Cell Responses and Their Role in Infectious Diseases. *J. Immunol. Res.* 2016. **2016**: 1–11. DOI: 10.1155/2016/2695396.
- 20 Walters, L.C., Harlos, K., Brackenridge, S., Rozbesky, D., Barrett, J.R., Jain, V., Walter, T.S. et al., Pathogen-derived HLA-E bound epitopes reveal broad primary anchor pocket tolerability and conformationally malleable peptide binding. *Nat. Commun.* 2018; **9**. DOI: 10.1038/s41467-018-05459-z.
- 21 McMurtrey, C., Harrieff, M.J., Swarbrick, G.M., Duncan, A., Cansler, M., Null, M., Bardet, W. et al., T cell recognition of Mycobacterium tuberculosis peptides presented by HLA-E derived from infected human cells. *PLoS One.* 2017; **12**. DOI: 10.1371/journal.pone.0188288.
- 22 Sylvester-Hvid, C., Kristensen, N., Blicher, T., Ferré, H., Lauemøller, S.L., Wolf, X.A., Lamberth, K. et al., Establishment of a quantitative ELISA capable of determining peptide - MHC class I interaction. *Tissue Antigens.* 2002. **59**: 251–8.
- 23 Toebes, M., Coccoris, M., Bins, A., Rodenko, B., Gomez, R., Nieuwkoop, N.J., Van De Kastelee, W. et al., Design and use of conditional MHC class I ligands. *Nat. Med.* 2006. **12**: 246–251. DOI: 10.1038/nm1360.
- 24 Bakker, A.H., Hoppes, R., Linnemann, C., Toebes, M., Rodenko, B., Berkers, C.R., Hadrup, S.R. et al., Conditional MHC class I ligands and peptide exchange technology for the human MHC gene products HLA-A1, -A3, -A11, and -B7. 2008. DOI: 10.1073/pnas.0709717105.
- 25 Brackenridge, S., Evans, E.J., Toebes, M., Goonetilleke, N., Liu, M.K.P., Di Gleria, K., Schumacher, T.N. et al., An Early HIV Mutation within an HLA-B*57-Restricted T Cell Epitope Abrogates Binding to the Killer Inhibitory Receptor 3DL1. *J. Virol.* 2011. **85**: 5415–5422. DOI: 10.1128/JVI.00238-11.
- 26 Garboczi, D.N., Hung, D.T. and Wiley, D.C., HLA-A2-peptide complexes: Refolding and crystallization of molecules expressed in *Escherichia coli* and complexed with single antigenic peptides. 1992.
- 27 Nielsen, M., Lundegaard, C., Worning, P., Lauemøller, S.L., Lamberth, K., Buus, S., Brunak, S. et al., Reliable prediction of T-cell epitopes using neural networks with novel sequence representations. *Protein Sci.* 2003. **12**: 1007–1017. DOI: 10.1110/ps.0239403.
- 28 Andreatta, M. and Nielsen, M., Gapped sequence alignment using artificial neural networks: Application to the MHC class I system. *Bioinformatics.* 2016. **32**: 511–517. DOI: 10.1093/bioinformatics/btv639.
- 29 Tomassec, P., Braud, V.M., Rickards, C., Powell, M.B., McSharry, B.P., Gadola, S., Cerundolo, V. et al., Surface expression of HLA-E, an inhibitor of natural killer cells, enhanced by human cytomegalovirus gpUL40. 2000. DOI: 10.1126/science.287.5455.1031.
- 30 Nattermann, J., Nischalke, H.D., Hofmeister, V., Kupfer, B., Ahlenstiel, G., Feldmann, G., Rockstroh, J. et al., HIV-1 infection leads to increased HLA-E expression resulting in impaired function of natural killer cells. *Antivir. Ther.* 2005. **10**: 95–107.
- 31 Jiang, H., Canfield, S.M., Gallagher, M.P., Jiang, H.H., Jiang, Y., Zheng, Z. and Chess, L., HLA-E-restricted regulatory CD8+ T cells are involved in development and control of human autoimmune type 1 diabetes. *J. Clin. Invest.* 2010. **120**: 3641–3650. DOI: 10.1172/JCI43522.
- 32 Jørgensen, P.B., Livbjerg, A.H., Hansen, H.J., Petersen, T. and Höllsberg, P., Epstein-Barr virus Peptide Presented by HLA-E is Predominantly Recognized by CD8bright Cells in multiple Sclerosis Patients Jacobson S, ed. *PLoS One.* 2012. **7**: e46120. DOI: 10.1371/journal.pone.0046120.
- 33 Thomsen, M.C.F. and Nielsen M., Seq2Logo; A method for construction and visualization of amino acid binding motifs and sequence profiles including sequence weighting, pseudo counts and two-sided representation of amino acid enrichment and depletion. *Nucleic Acids Res.* 2012; **40**. DOI: 10.1093/nar/gks469.
- 34 Miller, J.D., Weber, D.A., Ibegbu, C., Pohl, J., Altman, J.D. and Jensen, P.E., Analysis of HLA-E Peptide-Binding Specificity and Contact Residues in Bound Peptide Required for Recognition by CD94/NGG2. *J. Immunol.* 2003. **171**: 1369–1375. DOI: 10.4049/jimmunol.171.3.1369.
- 35 Walters, L.C., Harlos, K., Brackenridge, S., Rozbesky, D., Barrett, J.R., Jain, V., Walter, T.S. et al., Pathogen-derived HLA-E bound epitopes reveal broad primary anchor pocket tolerability and conformationally malleable peptide binding. 2018. DOI: 10.1038/s41467-018-05459-z.
- 36 Illing, P.T., Vivian, J.P., Dudek, N.L., Kostenko, L., Chen, Z., Bharadwaj, M., Miles, J.J. et al., Immune self-reactivity triggered by drug-modified HLA-peptide repertoire. *Nature.* 2012. **486**: 554–8. DOI: 10.1038/nature11147.

Abbreviations: β 2M: β -2 microglobulin · BCG: Bacillus CalmetteGuérin vaccine · BSA: Bovine serum albumin · CMV: Cytomegalovirus · EBV: Epstein-Barr virus · ELISA: Enzyme-linked immunosorbent assay · FPLC: Fast protein liquid chromatography · HCV: Hepatitis C virus · HIV: Human immunodeficiency virus · HLA-E: Human leukocyte antigen E · Mtb: Mycobacteria tuberculosis · PBS: Phosphate buffered saline · PPD: Purified protein derivative · Prdx5: Peroxiredoxin 5 · RhCMV: Rhesus Cytomegalovirus · SIV: Simian immunodeficiency virus · SD: Standard deviation · VL9: MHC class I leader sequence-derived signal peptide

Full correspondence: Prof. Geraldine M. Gillespie, Nuffield Department of Medicine Research Building, Roosevelt Drive, Nuffield Department of Medicine, University of Oxford, Oxford, OX3 7FZ, UK. Email: geraldine.gillespie@ndm.ox.ac.uk

Additional correspondence: Dr. Lucy C. Walters, Nuffield Department of Medicine Research Building, Roosevelt Drive, Nuffield Department of Medicine, University of Oxford, Oxford, OX3 7FZ, UK. Email: lucy.walters@ndm.ox.ac.uk

The peer review history for this article is available at <https://publons.com/publon/10.1002/eji.202048719>

Received: 4/5/2020

Revised: 19/6/2020

Accepted: 23/7/2020

Accepted article online: 27/7/2020